

# Self-oscillations in a superconducting stripline resonator integrated with a DC-SQUID

Eran Segev,\* Oren Suchoi, Oleg Shtempluck, and Eyal Buks  
 Department of Electrical Engineering, Technion, Haifa 32000, Israel  
 (Dated: December 11, 2018)

We study self-sustained oscillations (SO) in a Nb superconducting stripline resonators (SSR) integrated with a DC superconducting quantum interface devices (SQUID). We find that both the power threshold where these oscillations start and the oscillations frequency are periodic in the applied magnetic flux threading the SQUID loop. A theoretical model which attributes the SO to a thermal instability in the DC-SQUID yields a good agreement with the experimental results. This flux dependant nonlinearity may be used for quantum state reading of a qubit-SSR integrated device.

We study thermal instability in superconducting stripline resonators (SSR's) working at gigahertz frequencies. We have recently demonstrated how thermal instability can create extremely strong nonlinearity in such resonators<sup>1,2</sup>. This nonlinearity is manifested by self-sustained oscillations (SO) at megahertz frequencies, strong intermodulation gain, stochastic resonance, sensitive radiation detection, and more<sup>3</sup>. In the present work we have integrated a SSR with a DC superconducting quantum interface devices (SQUID). Similar configurations have been recently studied by other groups and it was shown that such devices can be used as readout and coupling elements for qubits<sup>4,5,6</sup>. In addition, it was shown that further improvement in the sensitivity of the readout process of the qubit is possible by biasing the resonator to a state of nonlinear responsivity<sup>5,6,7,8,9</sup>.

Our experiments are performed using the setup depicted in Fig. 1(a). We study the response of the integrated SSR to a monochromatic injected pump tone that drives one of the resonance modes, and measure the reflected power spectrum by a spectrum analyzer. We find that there is a certain range in the plane of the pump-frequency pump-power parameters, in which intrinsic SO occur in the resonator. These oscillations are manifested by the appearance of sidebands in the reflected power spectrum. In addition, we apply bias magnetic flux through the DC-SQUID and find that both the threshold where these oscillations start and their frequency are periodic in the applied magnetic flux, having a periodicity of one flux quantum. We extend our theoretical model<sup>1</sup>, which has originally considered SO and thermal instability in a SSR integrated with a single micro-bridge, to include this flux dependency and find a good agreement with the experimental results.

A simplified circuit layout of our device is illustrated in Fig. 1(b). We fabricate our devices on a Silicon wafer, covered by a thin layer of Silicon Nitride. Each device is made of a thin layer ( $< 100$  nm) of Niobium and composed of a stripline resonator having a DC-SQUID (1(c)) monolithically embedded into its structure. The resonator length is  $l = 18$  mm, and its first resonance mode is found at  $f_1 = \omega_1/2\pi = 3.006$  GHz. The DC-SQUID has two nano-bridges (1(d)), one in each of its two arms. Their size is typically  $100\text{ nm}^2$  and therefore each nano-bridge functions as a weak-link that approximately can

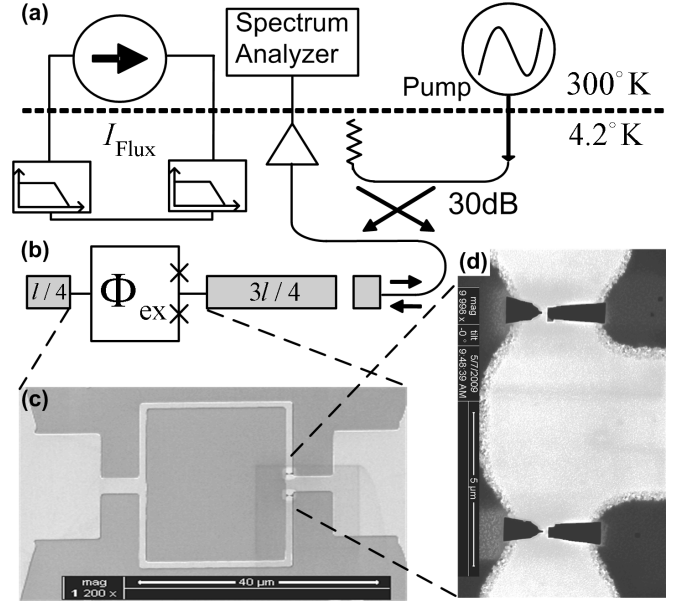


FIG. 1: (a) Measurement setup. (b) Schematic layout of our device. (c) SEM image of the DC-SQUID. (d) SEM image of the two nano-bridge-based Josephson junctions.

be regarded as a regular Josephson junction<sup>10,11</sup>. A feed-line, weakly coupled to the resonator, is employed for delivering the input and output signals. An on-chip filtered DC bias line passing near the DC-SQUID is used to apply magnetic flux through the SQUID. Some measurements are carried out while the device is fully immersed in liquid Helium, while others in a dilution refrigerator where the device is in vacuum. Further design considerations and fabrication details can be found elsewhere<sup>12</sup>.

Figure 2 exhibits SO in the power reflected off the resonator<sup>1,13</sup>. In this measurement we inject into the resonator an input pump tone having a monochromatic frequency  $\omega_p = \omega_1$ , and measure the reflected power spectrum around  $\omega_1$  while varying the input pump power  $P_p$ . At relatively low ( $P_p \lesssim -66$  dBm) and high ( $P_p \gtrsim -48$  dBm) pump powers the response of the resonator is linear, namely, the reflected power spectrum contains a single spectral component at the frequency of

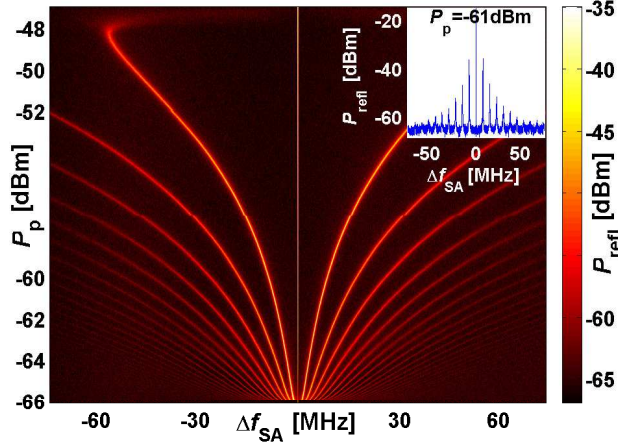


FIG. 2: Typical experimental results of the SO phenomenon. The color-map shows the reflected power  $P_{\text{refl}}$  as a function of the input pump power  $P_p$  and the measured frequency  $f_{\text{SA}}$ , centered on the pump frequency, which coincides with the first resonance frequency  $f_1$  ( $\Delta f_{\text{SA}} = f_{\text{SA}} - f_1$ ). Note that the data is truncated at  $P_{\text{refl}} = -35$  dBm for clarity. The inset shows a cut of that measurement obtained with  $P_p = -61$  dBm.

the stimulating pump tone. In between these two power thresholds the resonator self oscillates and regular modulation of the pump tone occurs. As a result, the reflected spectrum contains several orders of modulation products realized by rather strong and sharp sidebands (see inset of Fig. 2) that extend to both sides of the pump tone frequency. The SO frequency, defined as the frequency difference between the pump frequency and the primary sideband, ranges between few to tens of megahertz and increases with the pump power.

The dependence of the SO on the applied magnetic flux is shown in Fig. 3. In this measurement we inject a pump tone having a stationary frequency ( $\omega_p \simeq \omega_1$ ) and power ( $P_p = -51.5$  dBm), and measure the reflected power spectrum around  $\omega_1$  while varying the DC bias current. As shown, the SO frequency is periodically changed by the applied magnetic flux. The periodicity is one flux quantum and the relative change is typically about 20%. Figures 4(a) and (c) show two measurements of flux dependent SO obtained with pump power above and equal the threshold power ( $P_{p,(a)} = -51.5$  dBm,  $P_{p,(c)} = -51.6$  dBm), respectively. The later measurement demonstrates how magnetic flux can switch the resonator from a steady state response to a limit-cycle state where it experiences SO.

To account for our results we model our device as a transmission line resonator interrupted by a DC-SQUID. The impedance of the DC-SQUID is composed of a constant inductor in series with a flux-dependent inductor shunted by a parallel resistor<sup>12</sup>. The flux dependence of

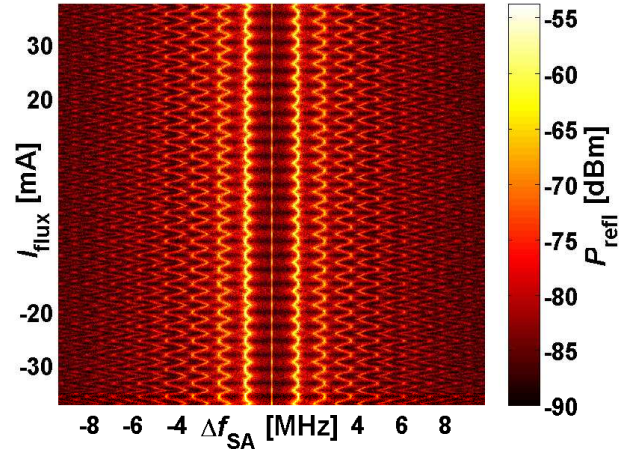


FIG. 3: Typical experimental results of flux dependent SO. The color-map shows the reflected power  $P_{\text{refl}}$  as a function of the bias DC current  $I_{\text{flux}}$  and the measured frequency  $f_{\text{SA}}$  centered on the pump frequency  $f_p = f_1$  ( $\Delta f_{\text{SA}} = f_{\text{SA}} - f_1$ ).

the DC-SQUID impedance gives rise to periodic dependence of the SSR's damping rates on the applied magnetic field (the change in the SSR resonance frequency is relatively small).

The dynamics of our system can be captured thus by two coupled equations of motion<sup>1</sup>. The first equation describes the dynamics of a resonator driven by feed-line carrying an incident coherent tone  $b^{\text{in}} = b_0^{\text{in}} e^{-i\omega_p t}$ , where  $b_0^{\text{in}}$  is constant complex amplitude and  $\omega_p = 2\pi f_p$  is the driving angular frequency. The mode amplitude inside the resonator can be written as  $B e^{-i\omega_p t}$ , where  $B(t)$  is complex amplitude, which is assumed to vary slowly on a time scale of  $1/\omega_p$ . In this approximation, assuming a noiseless system, the equation of motion of  $B$  reads<sup>14</sup>

$$\frac{dB}{dt} = [i(\omega_p - \omega_0) - \gamma] B - i\sqrt{2\gamma_1} b^{\text{in}}, \quad (1)$$

where  $\omega_0$  is the angular resonance frequency and  $\gamma(T) = \gamma_1 + \gamma_2(T, \Phi_{ex})$ , where  $\gamma_1$  is the coupling coefficient between the resonator and the feed-line and  $\gamma_2(T, \Phi_{ex})$  is the temperature and flux dependent damping rate of the mode.

The heat-balance equation for the temperature  $T$  of the nano-bridges composing the DC-SQUID is given by<sup>13</sup>

$$C \frac{dT}{dt} = 2\hbar\omega_0\gamma_2 |B|^2 - H(T - T_0), \quad (2)$$

where  $C$  is the thermal heat capacity,  $H$  is the heat transfer coefficient, and  $T_0$  is the temperature of the coolant.

Coupling between Eqs. (1) and (2) originates by the dependence of the damping rate  $\gamma_2(T, \Phi_{ex})$  of the driven mode on the impedance of the DC-SQUID<sup>15</sup>, which in turn depends on the temperature of its nano-bridges and on the applied magnetic flux. We assume a simple case,

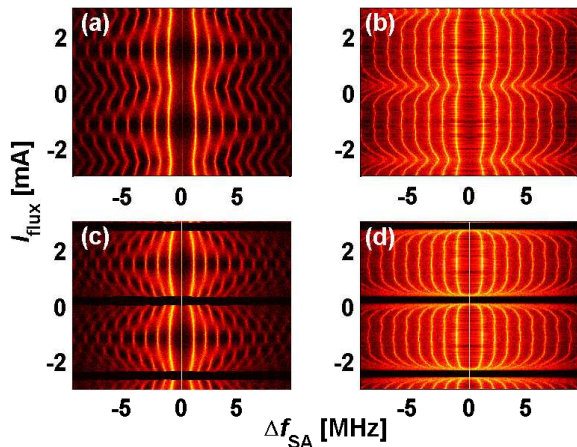


FIG. 4: Typical experimental and numerical results of flux dependent SO. Each panel shows a color-map of the reflected power  $P_{\text{ref}}$  as a function of the bias DC current  $I_{\text{flux}}$  and the measured frequency  $f_{\text{SA}}$  centered on the pump frequency  $f_p = f_1$  ( $\Delta f_{\text{SA}} = f_{\text{SA}} - f_1$ ). Panels (a) and (c) show experimental results obtained at pump power above and equals the low threshold power, respectively. Panels (b) and (d) show the corresponding theoretical results obtained by numerically integrating the equations of motion.

where the dependence on the temperature  $T$  is described by a step function that occurs at the critical temperature  $T_c$  of the superconductor. We further assume that only when the nano-bridges are in a superconducting phase the damping rate depends on the external flux. Namely,

$\gamma_2$  takes a flux dependent value  $\gamma_{2s}(\Phi_{ex})$  when the nano-bridges are in a superconducting phase ( $T < T_c$ ) and a flux-independent value  $\gamma_{2n}$  when they are in a normal-conducting phase ( $T > T_c$ ).

The results of a numerical integration of the equations of motion are shown in Fig. 4(b) and (d). Our model qualitatively reproduces the same flux dependency of the SM frequency on the magnetic flux. The parameters used for the numerical simulation were obtained as follows. The thermal heat capacity  $C = 4.5 \text{ nJ cm}^{-2} \text{ K}^{-1}$  and the heat transfer coefficient  $H = 24.5 \text{ mW cm}^{-2} \text{ K}^{-1}$  were calculated analytically according to Refs.<sup>16,17</sup>. The values of the resonance frequency and the various damping rates,  $\gamma_{1s} = 2.4 \text{ MHz}$ ,  $\gamma_{2s} \in [2.93, 3.32] \text{ MHz}$ ,  $\gamma_{2n} = 13 \text{ MHz}$ , and  $\omega_0 = 2\pi \cdot 3.006 \text{ GHz}$  were extracted from S11 reflection coefficient measurements according to<sup>18</sup>.

In conclusion, we report on periodic flux-dependency of SO in a SSR integrated with a DC-SQUID. The flux significantly modulates the oscillation frequency and can be used to turn them on and off if the device is driven near the power threshold. A theoretical model which attributes this behavior to thermal instability in the DC-SQUID exhibits a good quantitative agreement with the experimental results.

We thank Steve Shaw for valuable discussions and helpful comments. E.S. is supported by the Adams Fellowship Program of the Israel Academy of Sciences and Humanities. This work is supported by the German Israel Foundation under grant 1-2038.1114.07, the Israel Science Foundation under grant 1380021, the Deborah Foundation, the Poznanski Foundation, Russell Berrie nanotechnology institute, and MAFAT.

\* Electronic address: segev@tx.technion.ac.il

<sup>1</sup> E. Segev, B. Abdo, O. Shtempluck, and E. Buks, *J. Phys. Cond. Matt.* **19**, 096206 (2007).

<sup>2</sup> E. Segev, B. Abdo, O. Shtempluck, and E. Buks, *Phys. Rev. B* **77**, 012501 (2008).

<sup>3</sup> G. Bachar, E. Segev, O. Shtempluck, S. W. Shaw, and E. Buks, arXiv p. 0810.0964v2 (2008).

<sup>4</sup> A. Wallraff, D. I. Schuster, A. Blais, L. Frunzio, R.-S. Huang, J. Majer, S. Kumar, S. M. Girvin, and R. J. Schoelkopf, *Nature* **431**, 162 (2004).

<sup>5</sup> A. Lupacu, E. F. C. Driessen, L. Roschier, C. J. P. M. Harmans, and J. E. Mooij, *Phys. Rev. Lett.* **96**, 127003 (2006).

<sup>6</sup> J. C. Lee, W. D. Oliver, K. K. Berggren, and T. P. Orlando, *Phys. Rev. B* **75**, 144505 (2007).

<sup>7</sup> I. Siddiqi, R. Vijay, M. Metcalfe, E. Boaknin, L. Frunzio, R. J. Schoelkopf, and M. H. Devoret, *Phys. Rev. B* **73**, 054510 (2006).

<sup>8</sup> E. Boaknin, V. Manucharyan, S. Fissette, M. Metcalfe, L. Frunzio, R. V. I. Siddiqi, A. Wallraff, R. J. Schoelkopf, and M. Devoret (2007), arXiv:cond-mat/0702445v1.

<sup>9</sup> M. Metcalfe, E. Boaknin, V. Manucharyan, R. Vijay, I. Siddiqi, C. Rigetti, L. Frunzio, R. J. Schoelkopf, and M. H.

Devoret, *Phys. Rev. B* **76**, 174516 (2007).

<sup>10</sup> A. G. P. Troeman, S. H. W. V. der Ploeg, E. Il'ichev, H.-G. Meyer, A. A. Golubov, M. Y. Kupriyanov, and H. Hilgenkamp, *Phys. Rev. B* **77**, 024509 (2008).

<sup>11</sup> A. G. P. Troeman, H. Derking, B. Borger, J. Pleikies, D. Veldhuis, and H. Hilgenkamp, *Nano Lett.* **7**, 2152 (2008).

<sup>12</sup> O. Suchoi, B. Abdo, E. Segev, O. Shtempluck, M. P. Blencowe, and E. Buks, arXiv **0901.3110v1** (2009).

<sup>13</sup> E. Segev, B. Abdo, O. Shtempluck, and E. Buks, *Europhys. Lett.* **78**, 57002 (2007).

<sup>14</sup> B. Yurke and E. Buks, *J. Lightwave Tech.* **24**, 5054 (2006).

<sup>15</sup> D. Saeedkia, A. H. Majedi, S. Safavi-Naeini, and R. R. Mansour, *IEEE Microwave Wireless Compon. Lett.* **15**, 510 (2005).

<sup>16</sup> M. W. Johnson, A. M. Herr, and A. M. Kadin, *J. Appl. Phys.* **79**, 7069 (1996).

<sup>17</sup> K. Weiser, U. Strom, S. A. Wolf, and D. U. Gubser, *J. Appl. Phys.* **52**, 4888 (1981).

<sup>18</sup> E. Arbel-Segev, B. Abdo, O. Shtempluck, and E. Buks, *IEEE Trans. Appl. Superconduct.* **16**, 1943 (2006).